

## Salinity effects on the 2014 warm “Blob” in the Northeast Pacific

Hai Zhi<sup>1</sup>, Pengfei Lin<sup>2,3\*</sup>, Rong-Hua Zhang<sup>4</sup>, Fei Chai<sup>5,6</sup>, Hailong Liu<sup>2,3</sup>

<sup>1</sup> College of Atmospheric Sciences, Nanjing University of Information Science and Technology, Nanjing 210044, China

<sup>2</sup> State Key Laboratory of Numerical Modeling for Atmospheric Sciences and Geophysical Fluid Dynamics, Institute of Atmospheric Physics (IAP), Chinese Academy of Sciences, Beijing 100029, China

<sup>3</sup> College of Earth Sciences, University of Chinese Academy of Sciences, Beijing 100049, China

<sup>4</sup> Key Laboratory of Ocean Circulation and Waves, Institute of Oceanology, Chinese Academy of Sciences, Qingdao 266071, China

<sup>5</sup> State Key Laboratory of Satellite Ocean Environment Dynamics, Second Institute of Oceanography, Ministry of Natural Resources, Hangzhou 310012, China

<sup>6</sup> School of Marine Sciences, University of Maine, Orono 04469-5706, USA

Received 3 October 2018; accepted 21 January 2019

© Chinese Society for Oceanography and Springer-Verlag GmbH Germany, part of Springer Nature 2019

### Abstract

A significant strong, warm “Blob” (a large circular water body with a positive ocean temperature anomaly) appeared in the Northeast Pacific (NEP) in the boreal winter of 2013–2014, which induced many extreme climate events in the US and Canada. In this study, analyses of the temperature and salinity anomaly variations from the Array for Real-time Geostrophic Oceanography (Argo) data provided insights into the formation of the warm “Blob” over the NEP. The early negative salinity anomaly dominantly contributed to the shallower mixed layer depth (MLD) in the NEP during the period of 2012–2013. Then, the shallower mixed layer trapped more heat in the upper water column and resulted in a warmer sea surface temperature (SST), which enhanced the warm “Blob”. The salinity variability contributed to approximately 60% of the shallowing MLD related to the warm “Blob”. The salinity anomaly in the warm “Blob” region resulted from a combination of both local and nonlocal effects. The freshened water at the surface played a local role in the MLD anomaly. Interestingly, the MLD anomaly was more dependent on the local subsurface salinity anomaly in the 100–150 m depth range in the NEP. The salinity anomaly in the 50–100 m depth range may be linked to the anomaly in the 100–150 m depth range by vertical advection or mixing. The salinity anomaly in the 100–150 m depth range resulted from the eastward transportation of a subducted water mass that was freshened west of the dateline, which played a nonlocal role. The results suggest that the early salinity anomaly in the NEP related to the warm “Blob” may be a precursor signal of interannual and interdecadal variabilities.

**Key words:** warm “Blob”, mixed layer depth, surface and subsurface salinity anomalies

**Citation:** Zhi Hai, Lin Pengfei, Zhang Rong-Hua, Chai Fei, Liu Hailong. 2019. Salinity effects on the 2014 warm “Blob” in the Northeast Pacific. *Acta Oceanologica Sinica*, 38(9): 24–34, doi: 10.1007/s13131-019-1450-2

### 1 Introduction

Until recently, large-scale climatic events and related extreme climate responses were observed in association with climate change under global warming (Yoon et al., 2015). For example, during the boreal winter of 2013/2014, sea surface temperature (SST) was remarkably warm in the Northeast Pacific (NEP, 40°–50°N, 155°–140°W) and the SST body was circular with a large spatial extent (Freeland and Whitney, 2014). During the subsequent 23 months, the entire NEP remained significantly warmer by several degrees than during any other time in the last few decades. Thus, this SST anomaly was named the warm “Blob” (Freeland and Whitney, 2014; Bond et al., 2015). The record-breaking warm SST anomaly (SSTA) in the NEP and the associated processes induced many extreme weather events in Canada and the U.S. during the winter of 2013/2014 (Blunden and Arndt, 2015; Hartmann, 2015; Williams et al., 2015). Thus,

this striking climate event has attracted much attention in the scientific community (Palmer, 2014; Wang et al., 2014; Yu and Zhang, 2015; Baxter and Nigam, 2015; Kintisch, 2015; van Oldenborgh et al., 2015; Tseng et al., 2017). In particular, the processes responsible for the SST variability were crucial for a complete understanding of the climate variability and the related physics. It is important to provide insights into the effects of the anomalous warm ocean conditions under global warming in the future.

Salinity, as a fundamental variable responsible for seawater density, is governed by surface and subsurface forcings, ocean advection, mixing and so on (e.g., Fedorov et al., 2004; Huang and Mehta, 2005; Zhang et al., 2010). Additionally, salinity change can in turn modify the oceanic temperature by affecting the ocean stratification vertical distribution (Zhang et al., 2015). Is this extreme oceanic climate event, the warm “Blob”, linked to the salinity anomaly associated with freshwater flux?

Foundation item: The National Key Research and Development Program for Developing Basic Sciences under contract Nos 2016YFC1401601 and 2016YFC1401401; the National Natural Science Foundation of China under contract Nos 41376026, 41690122, 41690120 and 41475101; the NSFC-Shandong Joint Fund for Marine Science Research Centers under contract No. U1406401; the NSFC Innovative Group Grant under contract No. 41421005; the Taishan Scholarship.

\*Corresponding author, E-mail: [Linpf@mail.iap.ac.cn](mailto:Linpf@mail.iap.ac.cn)

The purpose of this study is to explore the formation processes of the warm “Blob” associated with the salinity variability effects on the mixed layer salinity. Our two-fold analyses aim to (1) identify the relationship among the warm “Blob”, salinity anomaly (SA) and related physics; (2) identify the contribution of the SA to the warm “Blob”; and (3) determine the possible mechanism for the SA associated with the warm “Blob”. The remainder of this paper is organized as follows. In Section 2, the data and methodology are described. In Section 3.1, the spatial structures and temporal evolution of the SSTA and SA are presented. In Section 3.2, the oceanic physics are examined to determine the exact relationship between the ocean salinity and “Blob”, and the possible mechanism of the warm “Blob” formation is deduced. In Section 3.3, the possible mechanisms responsible for the salinity variations are discussed. In Section 4, the mechanism responsible for the “Blob” is summarized, and the relationship between the SA and this extreme climate event is discussed.

## 2 Data and method

The following observational and reanalysis datasets were used in this study. The precipitation data were obtained from the Global Precipitation Climatology Project (GPCP) dataset (Version 2), covering the period of January 1979 to October 2015 with a  $2.5^\circ \times 2.5^\circ$  horizontal resolution (Adler et al., 2003). The monthly evaporation data were derived from the Objectively Analyzed Ocean-Air Fluxes (OAFflux) dataset (Yu et al., 2008) from 1958 to present in an even horizontal grid of  $1^\circ \times 1^\circ$ . The gridded ocean salinity and temperature datasets were acquired from the Array for Real-time Geostrophic Oceanography (Argo) provided by the International Pacific Research Center (IPRC)/Asia-Pacific Data-Research Center (APDRC) (<http://apdrc.soest.hawaii.edu/projects/argo/>), with monthly and long-term climatology fields spatially averaged within  $1^\circ$  bins from 5 to 2 000 m depth covering the period from 2005 to present. The mixed layer depth (MLD) and isothermal layer depth (ILD) were also directly provided by the ARGO dataset. The climatological anomalies in the study were calculated relative to the climatological monthly mean from January 2005 to December 2015. All the data were interpolated on the  $1^\circ \times 1^\circ$  grids to match the ARGO dataset.

In this study, key oceanic fields, including the MLD and ILD, were determined using the 3-dimensional salinity and temperature fields. The ILD was calculated as the depth where the temperature  $\Delta T$  was lower than that at the 10 m depth, where  $\Delta T = 0.2^\circ\text{C}$ . MLD was calculated as the depth where the density was  $\Delta\rho$  higher than that at 10 m depth.  $\Delta\rho$  was the value equivalent to the temperature decrease in  $0.2^\circ\text{C}$  (Kara et al., 2000). In addition, BLT was defined as the difference between the MLD and ILD when the MLD was shallower than the ILD (Sprintall and Tomczak, 1992; de Boyer Montegut et al., 2004; Bosc et al., 2009). The same approach provided in the Argo data was adopted for calculation of the MLD and ILD in this study.

To isolate the contributions of temperature and salinity to the MLD (using the density criteria) associated with the warm “Blob” in the NEP, an analysis was performed following Zheng and Zhang (2012) in determining the MLD anomaly. The density field was a function of temperature ( $T$ ) and salinity ( $S$ ), defined as  $F(T, S)$ . The interannual variation in density can be attributed to the temperature and/or salinity. Then, the relative effects of the climatological or interannual varying temperature and salinity fields on the interannual density anomaly can be estimated individually.

## 3 Results

### 3.1 Salinity variations associated with the warm “Blob”

A large circular SSTA body was found in January 2014 in the NEP by removing the multiyear climatological monthly mean SST (2005–2015). The most striking feature was that a large mass of warm water increased obviously and the SSTA magnitude was exceeding 3 standard deviations above the normal value in the area ( $40^\circ\text{--}50^\circ\text{N}$ ,  $155^\circ\text{--}140^\circ\text{W}$ ) in January 2014 (Bond et al., 2015). The warm anomaly was named the warm “Blob”, which is centered at  $42^\circ\text{N}$ ,  $148^\circ\text{W}$  (Fig. 1a). In January 2014, the area and intensity of this warm anomaly reached the maximum. Such an SSTA and its large extension were without precedent in the historical record. Furthermore, the SSTA was associated with a large SA prior to the warm “Blob” in the NEP (Figs 1b–e). The negative SA in the upper 100 m existed from January 2012 to January 2014, and a negative peak ( $< -0.2$ ) occurred in the winter of 2012–2013 in the NEP (Fig. 2b). Although a large SA was positive in the southwest part of the warm “Blob”, a fresh anomaly remained in the northeast part in January 2014 (Figs 1c and e).

There were several obvious anomalous physical fields related to the warm “Blob” in the NEP. During the 2012–2015 period, the regionally averaged time-depth profiles, including temperature, salinity and MLD anomalies, are shown in Fig. 2. The peak of the positive ocean temperature anomaly in the near upper 100 m layer was greater than  $2.5^\circ\text{C}$  in January 2014 (Fig. 2a). Notably, in late 2014, the positive ocean temperature anomaly had extended downward to a depth of 200 m. A significant amount of heat was stored in the ocean subsurface. Interestingly, the sea surface SA (SSSA) followed the SSTA evolution exactly, which had a similar sign to the SSA and both presented decadal variations from 2005 to 2015. The negative SA first appeared in the spring of 2012 and lasted until the spring of 2014. The maximal SA reached  $-0.2$  in the depth range of 100–150 m in the winter of 2012 (Fig. 2b). Specifically, the negative SA peak led the peak of the warm “Blob” by approximately 12 months. From the spring of 2014, the negative SA attenuated and then shifted into a positive anomaly, and the maximal positive anomaly ( $>0.5$ ) also occurred in the depth range of 100–150 m in the spring of 2015 in the warm “Blob”.

Corresponding to the SSTA evolution, the surface and subsurface salinities at the 100 m depth anomaly (i.e., SSSA and SSA100) averaged in the warm “Blob” are shown in Fig. 2c. During the 2005–2013 period, the correlation coefficient between the SSA 100 was as high as 0.87 in the warm “Blob”. The covaried relationship presented some differences including the amplitude and tendency during the 2014–2015 period. For example, the SA amplitude was greater than that at the surface. However, the salinity anomalies led the SSTA by approximately 12 months. The corresponding correlation between the SSTA and SSSA or SSA100 was significantly negative from January 2012 to January 2014. Thus, both the subsurface and negative surface salinity anomalies may have contributed to the development of the warm “Blob” by affecting the stratification.

The MLD revealed a shallow trend from 2010 to 2014 with obvious interannual variations in the warm “Blob” region (Fig. 2d). The MLD was very shallow (MLD anomaly  $< -10$  m) during 2013–2015, reaching the minimum, which was different from the climatology during 2005–2015. The relationship between MLD minimum and extreme warm events in the warm “Blob” region suggests that the development of the warm “Blob” may be related to the salinity variation and in particular, to the stratification due to the SA.

To explore whether the SSSA or SSA was more related to the

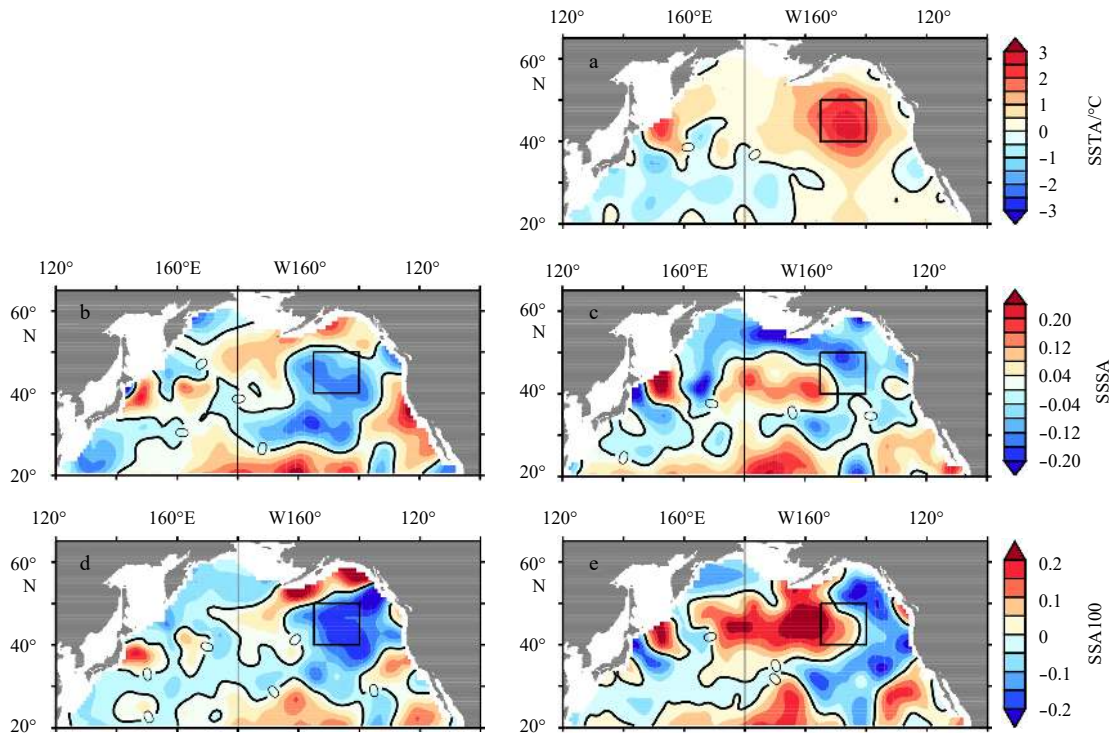


**Fig. 1.** Sea surface temperature anomaly (SSTA) (a), sea surface SA (SSSA) (c) and sea SA at the depth of 100 m (SSA100) (e) in January 2014; and SSSA (b) and SSA100 (d) in February 2013. The anomaly is calculated relative to the monthly climatological mean during January 2005 to December 2015. The thick black box denotes the center region of the warm “Blob” (40°–50°N, 155°–140°W).

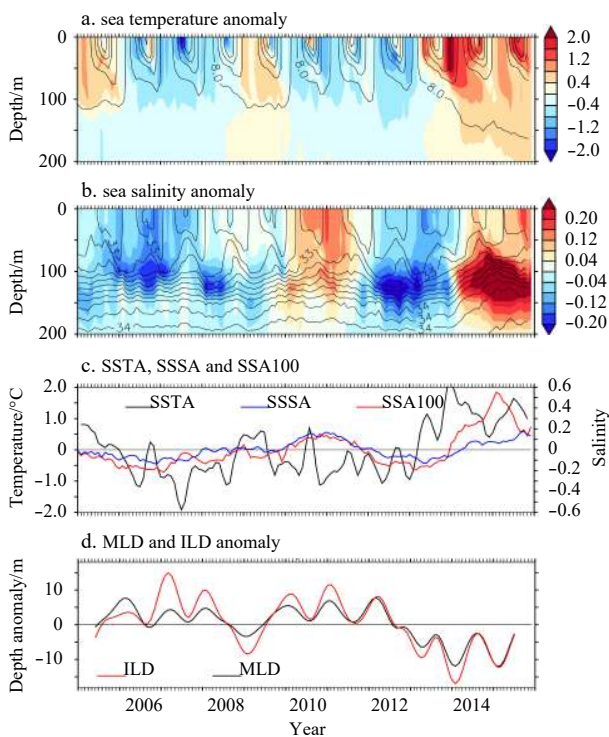


**Fig. 2.** The time-depth profiles of the regionally averaged temperature (a) and salinity (b) anomalies in the warm “Blob” (in the black box in Fig. 1). The time series of SSTA, SSSA and SSA100 (c) and interannual MLD and ILD (d) anomalies of the regional mean in the warm “Blob” (indicated by the box shown in Fig. 1).

temporal and spatial changes in the SSTA, the evolutions of the SSTA, SSSA, SSA and MLD anomalies during the 2012–2013 period are shown in Fig. 3. A positive SSTA first appeared in the Northwest Pacific during 2012, and then exceeded 1.0°C in August. Near the dateline of the northern Pacific, the positive SSTAs increased continuously after April 2013. Then, the SSTAs in the NEP began to increase and reached approximately 0.8°C in August 2013. The warm anomalies developed in the other regions. One anomaly was located along the Kuroshio Extension and southwest of the Bering Sea, and another anomaly was off the coast of Baja, California. Subsequently, the two warm SSTs merged together, possibly by the oceanic transport. In December 2013, the warm “Blob” showed a circular form and had nearly reached maturity.

In addition, in the warm “Blob” region, the SSSA and SSA100 remained negative from April 2012 to December 2013 (second and third columns in Fig. 3). A low surface SA appeared in April 2012. The low surface SA was enhanced and was much more significant from August 2012 to December 2012. The low SA was transported eastward and northward by Ekman transport. The enhanced salinity signal was mainly from the area southwest of the warm “Blob”. The low surface anomalies reached minimal values in April 2013. Notably, the fresh anomaly in the warm “Blob” became weak in August and December 2013 since the freshwater mass continued to move eastward and moved out of the warm “Blob” region. The SSA100 was more obvious than the surface fresh anomaly. From April 2012 to April 2013, the fresh anomaly became obvious. Subsequently, the fresh water was transported northeastward and weakened in August 2013 and December 2013. The origin of the fresh source may be traced to the fresh anomaly from the west or southwest.

Both the temperature and salinity variabilities can change the

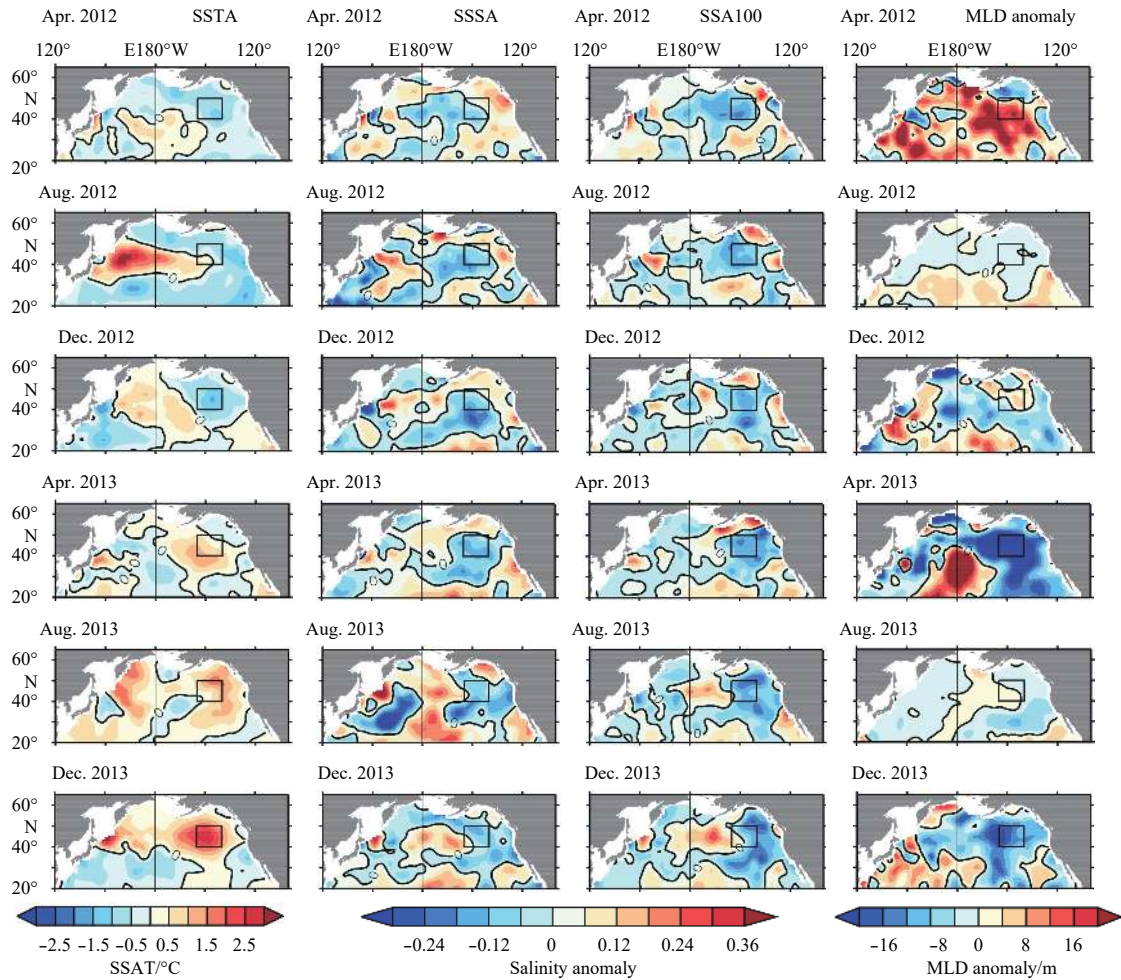


**Fig. 3.** The spatial evolutions of the SSTA (first panels), salinity anomalies at the surface (second panels) and 100 m (third panels), and the MLD (fourth panels) from April 2012 to December 2013 with an interval of 4 months.

MLD, such that the high temperature or low salinity seawater can shallow the MLD. Notably, in April 2013, the MLD became shallow, which was obviously due to the warm and low salinity water at the depth of 150 m. The negative MLD anomaly covaried with the negative SA. The SSTA changed from negative to positive and reached the positive peak despite that a lagged SA at 12 months. Thus, a hypothesis was proposed that the negative SA from January 2012 to December 2013 contributed to the shallow MLD and then enhanced the warm SST in the warm “Blob” region.

### 3.2 Salinity anomaly contributions to the warm “Blob”

According to the conventional theory, both the warm water and low salinity of the upper ocean can make the MLD shallow. To clearly distinguish the contribution to the MLD variability from the salinity and temperature variability, a diagnostic method proposed by Zheng and Zhang (2012) is used. This method was used to analyze the BLT and related oceanic stratification in the El Niño-Southern Oscillation (ENSO) cycle (Zhang and Busalacchi, 2009; Zheng et al., 2014).

Corresponding to the negative salinity peak in the warm “Blob”, the mean spatial distributions of the MLD anomaly in February 2013 are shown in Fig. 4. The climatological monthly mean MLD was already subtracted, which was calculated by the climatological monthly mean temperature and salinity, i.e.,  $T_{\text{clim}}$  and  $S_{\text{clim}}$ , respectively.  $T_{\text{inter}}$  and  $S_{\text{inter}}$  represented the interannu-

al temperature and salinity fields, respectively, which were used for the MLD calculation. The MLD calculated by the density criteria was the same as that directly derived from the Argo products (not shown). In Fig. 4a, both the interannual temperature and interannual salinity were used in the MLD calculation. The MLD anomaly was negative in the warm “Blob”, which meant the MLD was shallower than that using the climatological monthly mean temperature and salinity. In the warm “Blob” region, the averaged MLD shallowed to approximately 9.3 m considering the effects of the interannual variations in temperature and salinity (Table 1, denoted total MLD anomaly in the following). Considering only the effects of the interannual variation in temperature (Fig. 4b), the MLD shallowed to 8.0 m in the warm “Blob”. The correlation coefficient between the MLD anomaly considering the interannual variations in both temperature and salinity and only the temperature interannual variation was 0.87 (Table 2). The relationship indicated the important contribution of the interannual variations in temperature to the total MLD anomaly (–87.5%, Table 1). When considering only the effects of the interannual variation in salinity (Fig. 4c), the averaged MLD shallowed to approximately 5.8 m in the warm “Blob”. The contribution of the interannual salinity variation to the total MLD anomaly was 62.3% (Table 1). Therefore, the contribution of the interannual salinity to the total MLD anomaly was significant in the warm “Blob”. This salinity variation contribution to the MLD was

mainly due to the larger salinity effect on density in the special temperature-salinity environment, based on the salinity-temper-

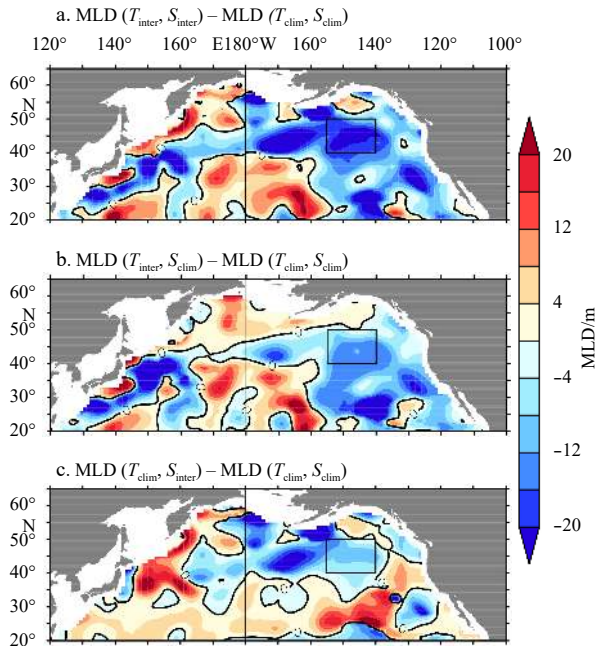


**Fig. 4.** The spatial distributions of the MLD anomaly in the northern Pacific in February 2013, which correspond to the prior period of the negative salinity peak. The MLD is calculated by the monthly mean temperature and salinity with an interannual variation ( $T_{inter}, S_{inter}$ ) (a), by the monthly mean temperature and monthly climatological mean salinity ( $T_{inter}, S_{clim}$ ) (b) and by the monthly temperature and monthly climatological mean salinity ( $T_{clim}, S_{inter}$ ) (c). All three of these MLD anomalies were deducted from the climatological monthly MLD field using the monthly climatological mean temperature and salinity ( $T_{clim}, S_{clim}$ ).

**Table 1.** The mixed layer depth (MLD) anomaly calculated by different combinations (interannual or climatologically monthly mean) of temperature and salinity relative to the MLD, which is calculated using monthly climatological mean temperature and salinity from February 2013 to display the contribution of changing temperature or salinity

	MLD anomaly/m	Contribution
MLD ( $T_{inter}, S_{inter}$ )	-9.27	
MLD ( $T_{inter}, S_{clim}$ )	-8.04	87.5%
MLD ( $T_{clim}, S_{inter}$ )	-5.77	62.3%

ature relationship.

The salinity contribution to the MLD change not only appeared in January 2014 but also in the most recent decade (2005–2015). As seen in the time series of the MLD averaged in the warm “Blob” during the 2005–2015 period (Fig. 5), there were close relationships between the total MLD anomaly, i.e., due to ( $T_{inter}, S_{inter}$ ), and MLD anomaly due to only the interannual salinity ( $T_{clim}, S_{inter}$ ) or interannual temperature ( $T_{inter}, S_{clim}$ ). The MLD anomaly due to the combination ( $T_{clim}, S_{inter}$ ) exerted an obvious contribution to the total MLD anomaly, such as during the winters of 2010, 2011 and 2012. In Table 2, the correlation between the MLD anomaly due to the combination ( $T_{clim}, S_{inter}$ ) and the combination ( $T_{inter}, S_{inter}$ ) was significantly high ( $-0.75$ ), although the correlation between the MLD anomaly due to the combination ( $T_{inter}, S_{clim}$ ) and total MLD anomaly was slightly high ( $R=0.87$ ). Those correlations indicated that the MLD anomaly can be greatly affected by the salinity interannual salinity variation.

In addition to the surface, the obvious negative SA was also located in the depth range of 50–100 m during the winter of 2012–2013 (Fig. 2). Did such a salinity anomaly contribute to the MLD anomaly in the warm “Blob”? The same method used in Fig. 4 was used to distinguish the individual effects of the SA on MLD anomaly at different depths. Hence, the MLDs were calculated by replacing the interannual salinity variation in only the upper 0–50 m layer (denoted FirD) and 50–100 m layer (denoted SecD). Both MLDs were compared using the climatological monthly mean temperature and salinity. The MLD differences due to salinity variations in those two layers are provided in Fig. 6. The relative effects of FirD and SecD were regionally dependent (Figs 6b, c). The MLD anomaly calculated by the SecD presented remarkable negative values, whereas the MLD calculated by the FirD presented slightly negative values. Therefore, the effects of the SecD played an important role in the shallowing MLD in the warm “Blob”. For the warm “Blob” event, the negative SA on the SecD exerted a larger contribution to shallowing the MLD than that of the SA contribution to the FirD. In fact, the most obvious SA was located in the depth range of 100–150 m. This SA can connect with the SA at the depth range of 50–100 m by vertical mixing during boreal winter (Fig. 2).

### 3.3 Causes of the SA associated with the warm “Blob”

Through the above analyses, it was confirmed that the effect of the subsurface SA in the deeper layer was an important factor in enhancing the warm “Blob” by modulating the upper ocean stratification. Therefore, to trace the SA source, the longitude-time profiles of the SSTa, SSSa and SSA100 averaged between

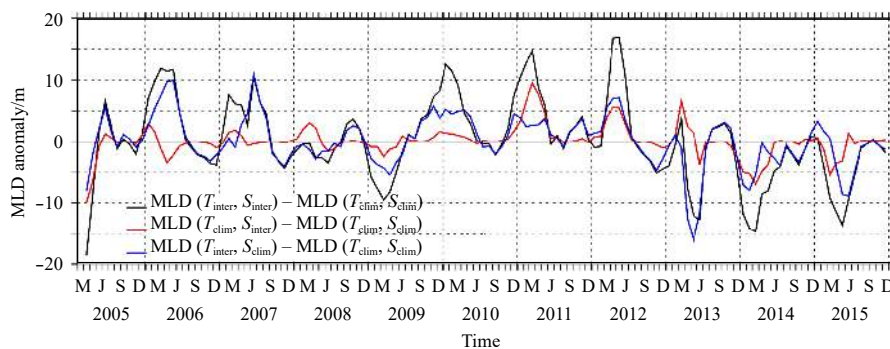


**Fig. 5.** The MLD time series calculated by ( $T_{inter}, S_{inter}$ ), ( $T_{inter}, S_{clim}$ ) and ( $T_{clim}, S_{inter}$ ) in the box ( $40^{\circ}$ – $50^{\circ}$ N,  $155^{\circ}$ – $140^{\circ}$ W) from 2005 to 2015. Units are meters for MLD. M represents March, J June, S September, and D December.

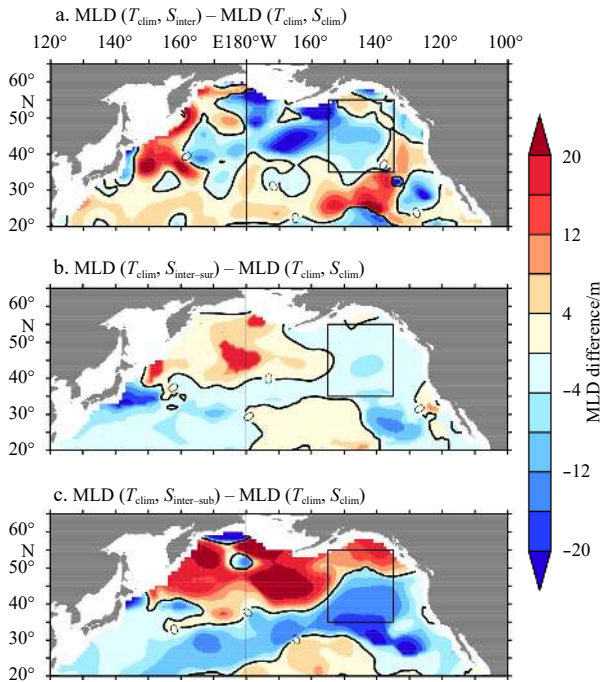


**Fig. 6.** The MLD difference between the monthly climatological mean temperature ( $T_{\text{clim}}$ ) and monthly mean salinity (with inter-annual variation) ( $S_{\text{inter}}$ ) (a), monthly climatological temperature ( $T_{\text{clim}}$ ) and salinity except the surface salinity (0–50 m) is the monthly mean (b) and monthly climatological temperature ( $T_{\text{clim}}$ ) and salinity except the subsurface salinity (50–100 m) (c) is the monthly mean. All three MLD anomalies were deducted from the climatological monthly MLD field using monthly climatological mean temperature and salinity ( $T_{\text{clim}}, S_{\text{clim}}$ ). Units are meters for MLD.

40°N and 50°N are presented in Fig. 7. As shown in Fig. 7, the stronger SSTA associated with the warm “Blob” did not present an obvious eastward propagation (Fig. 7a), meaning that the SSTA associated with the warm “Blob” was caused by the local effect, which can increase the amount of heat in the upper ocean. Notably, for the SSSA and SSA100, the eastward propagations were obvious in Figs 7b and c. The negative SSSA related to the warm “Blob” in January 2014 originated from the west coast of the northern Pacific in December 2010. A low SSS first appeared in December 2010 and reached the NEP in December 2012, and then, the low SSS stalled in that location until the warm “Blob” event occurred. The SSA100 also presented an obvious eastward propagation along this latitude. The SA in the deeper layer was more significant than the anomalies at the surface east of the dateline. The significant signal first appeared near the dateline in December 2011. The SA in the deeper layer might result from the subduction close to the westward boundary because the local surface SA was fresher. As shown in the evolution of the fresh water flux (FWF: evaporation (E) minus precipitation (P)) anomaly (Fig. 8a), there was a negative FWF anomaly near the westward boundary from July to December 2010. Regionally, the negative FWF anomaly induced the obvious low surface salinity. The low SSSA subducted into the subsurface and advected eastward. The SSSA subduction at the latitude of ~40°N north of the Kuroshio Extension region, as described by Liu and Huang (2012), could induce the SSA100 anomaly near the dateline by advection of the fresh water mass. Therefore, both the SSSA and SSA100 were en-

hanced by the FWF anomaly after December 2012, and then, the shallower MLD was enhanced beginning in 2013 (Fig. 8b).

### 3.4 Trace of FWF related to the SA of the warm “Blob”

The aforementioned analyses elucidated the effects of the SA on the warm “Blob”, and the related subsurface SA mainly depended on the FWF anomaly. However, where did the fresh water mass related to the SA originate? To explore the possible origin and propagation of the fresh water related to the warm “Blob”, the horizontal distributions of the leading correlation coefficients (denote  $r$ ) between the SSSA, SSA100 and FWF anomalies with the SSA100 averaged in the warm “Blob” are presented in Fig. 9.

As seen in the left and middle panels of the correlation maps between the SSA100 and SSSA with the SSA100 in Fig. 9, the positive correlations were located in the belt between 40°–50°N near the dateline, east of Japan and in the eastern Pacific south of 30°N in the 30-month to 24-month leading correlation maps. The positive correlations were moving from west and south of the warm “Blob” in the 18 to 4-month leading correlation maps. Then, the positive correlations between the SSA100 and SSSA suggested that the quasibarotropic structures of the SA existed in the upper 150 m prior to the mature period of the warm “Blob”.

Combined with the leading correlation between the FWF anomaly and SSA100, the positive correlations were located east of Japan and in the eastern Pacific south of 30°N in the 36-month, 30-month and 24-month leading correlation maps, respectively (the right panels in Fig. 9). The FWF anomalies east of Japan at approximately 40°N and the eastern Pacific south of 30°N were the possible sources resulting in the SSA100 and SSSA, and subsequently, the SSA100 and SSSA were transported by ocean advection into the warm “Blob” region. Moreover, the significant positive correlation was located near the dateline in the 8-month and 4-month leading correlation maps of the FWF anomaly. This finding indicated that the FWF anomaly can affect the SA, which enhances the negative SA. Notably, the obvious high leading correlation of the FWF anomaly was located further northward than that of the SSA or SSSA (i.e., in the Kuroshio Extension east of Japan). Therefore, we can conclude that the FWF anomaly induced the SSSA, and then, the SSSA was quickly advected to the Kuroshio Extension by the western boundary current before the appearance of warm “Blob” event. Near the dateline of the northern Pacific, the anomalous freshened water mass subducted into the subsurface layer in the depth range of 100–150 m and reached the region of the warm “Blob”.

To trace the source and evolution of the FWF anomaly related to the warm “Blob”, Fig. 10 shows the distributions of the leading correlation between the P/E anomaly and SSA in the warm “Blob”, respectively. As shown in Fig. 10, the E anomaly can contribute to the SA in the Kuroshio Extension east of Japan due to the positive correlation in the 36–18 month leading correlation. This finding suggests that the high E anomaly can lead to the high positive SA, and vice versa. However, the  $r$  was negative in the 36–30 month leading correlation, as shown in the right panels of Fig. 10, which indicated that the positive P anomaly can cause the negative SA. These relationship patterns suggest that the positive P and negative E anomalies can contribute to the negative FWF anomaly and the negative SA in the Kuroshio Extension east of Japan for the leading 36–30 months. Only the E anomaly can contribute to the FWF anomaly and SSA in the Kuroshio Extension east of Japan in the leading 24–18 month correlations.

In the eastern Pacific south of 30°N, the P anomaly contrib-

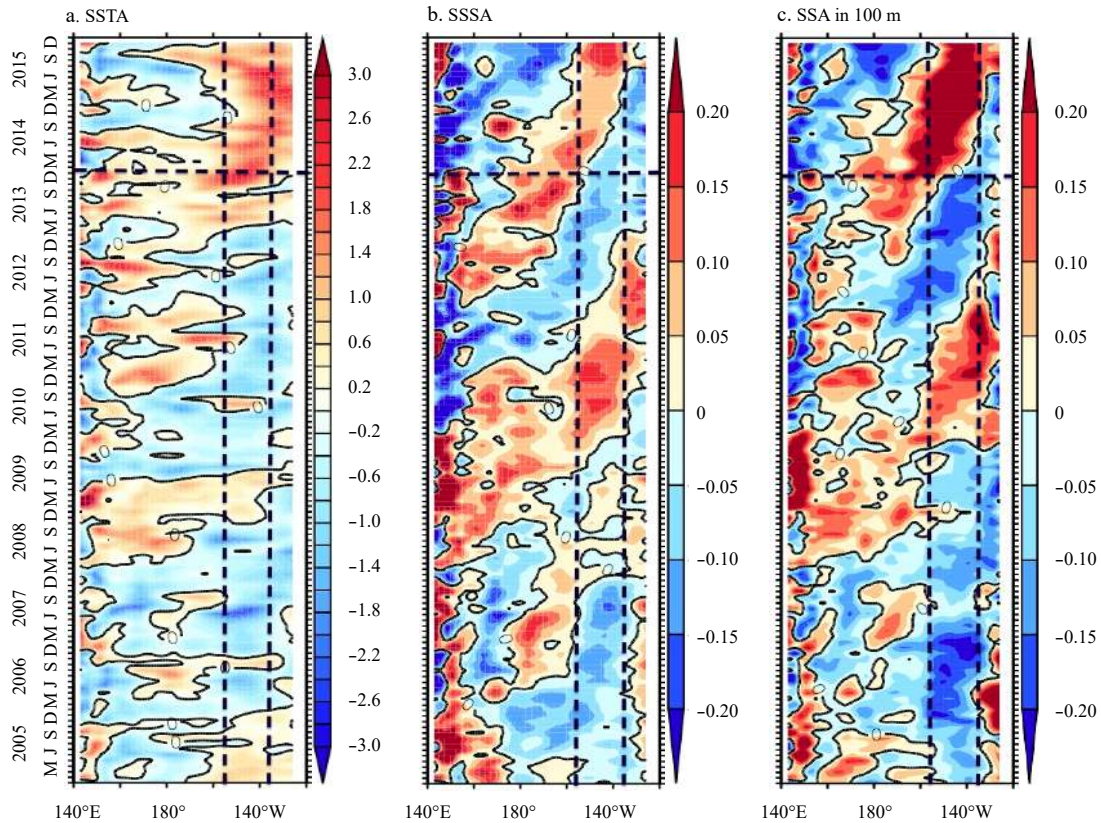


**Fig. 7.** Longitude-time sections along 120°W–140°E in the northern Pacific (averaged between 40°N and 50°N) for SSTA (°C) (a) and SSSA (b); and the SSA100 derived from the ARGO data (c). The two vertical dotted lines denote the warm “Blob”, and the horizontal dotted line denotes the date in January 2014. M represents March, J June, S September, and D December.

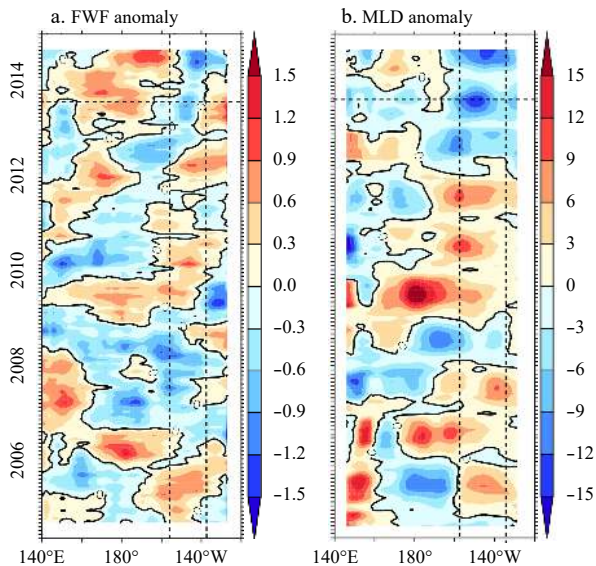


**Fig. 8.** Longitude-time sections along 120°W–140°E in the northern Pacific (averaged between 40°N and 50°N) for the FWF anomaly (10<sup>-6</sup> m/s) (a) and MLD anomaly (m) (b) during 2005–2015. The thick dark dashed lines indicate the meridional position and timing of the warm “Blob”.

uted more to the FWF anomaly due to the negative correlations in the leading 36–24 months (right panel in Fig. 10), which is in contrast to the positive correlation in the E anomaly maps (left

panel in Fig. 10). From the leading 18–0 months, the correlations (negative) of the P anomaly were more significant than those (positive) of the E anomaly, especially near the dateline along 40°–50°N. This finding suggests that the P anomaly maintained the SA in the depth range of 100–150 m. Thus, the SSTA in the warm “Blob” was associated with the ocean-atmosphere interactions of local and nonlocal oceanic processes. Notably, the negative FWF anomaly in the Northwest Pacific resulted in a positive P anomaly, which led to the negative SA. Furthermore, the negative SA (low salinity) was strengthened by more precipitation during the eastward propagation of the low salinity mass.

#### 4 Summary and discussion

An unprecedented and remarkable warm anomaly occurred in the NEP in January 2014. Despite the occurrence of extreme weather events and climate anomalies in several regions, this warm anomaly can provide us with an opportunity to explore the climate variability in the NEP. Until recently, the mechanisms, dynamics and full consequences of the climate anomaly were still being assessed. A growing consensus about the dominant contributing factors to the warm “Blob” development in the NEP has been attained, and the awareness of the “Blob”’s significance is growing. In this paper, based on the Argo three-dimensional salinity and temperature data, the effect of salinity on the warm “Blob” in the NEP (which appeared during the winter of 2013/2014) was investigated. This study has brought new insights to the understanding of climate change under global warming.

Due to the obvious SA associated with the SSTA, the warm “Blob” in the NEP in January 2014 can be described as the feed-

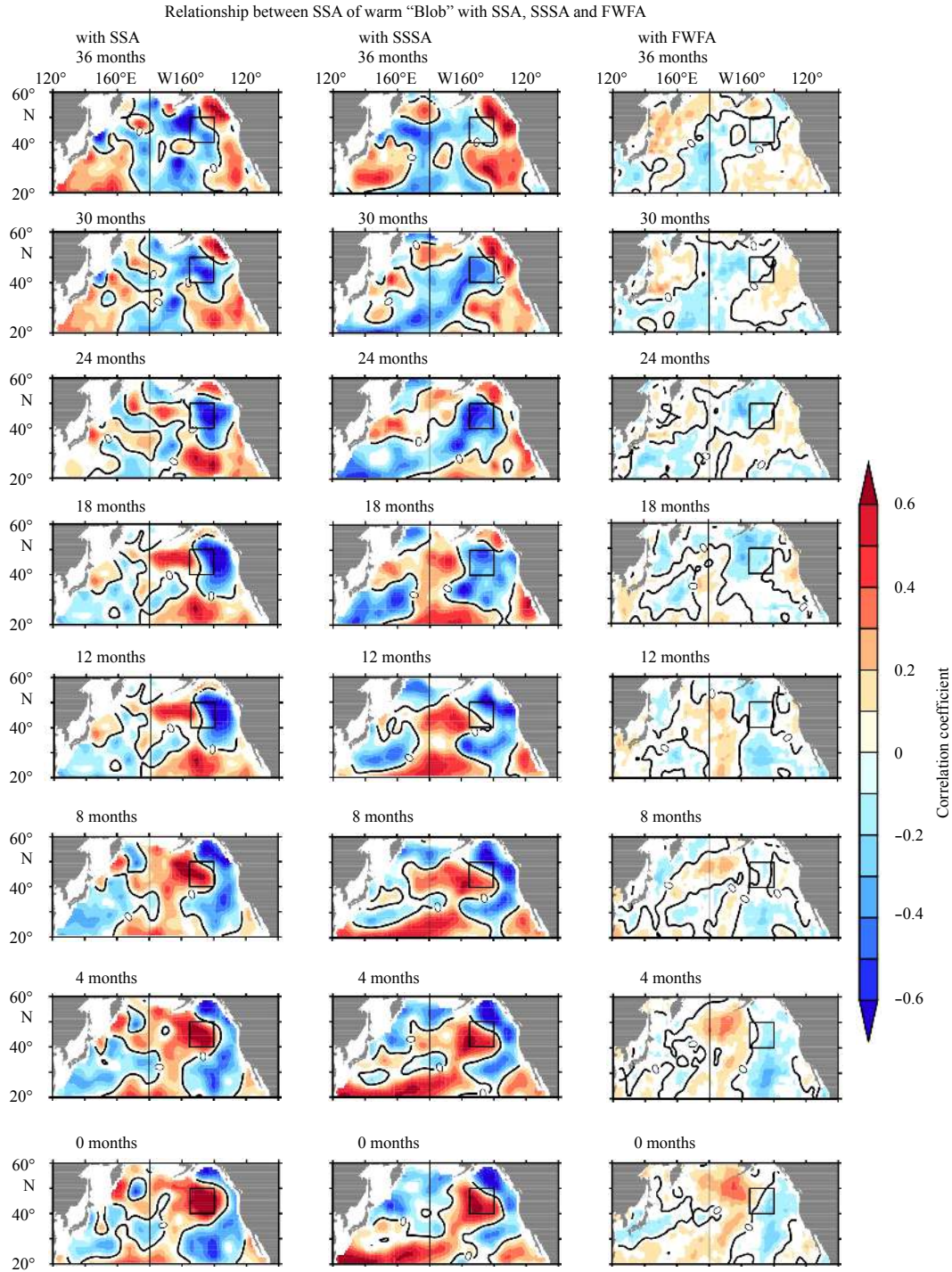


**Fig. 9.** The spatial distributions of the correlation coefficients showing that the FWF leads the SSA100 averaged in the center of the warm "Blob" from 36–0 months (left panels); the middle panels are same as the left panels, but for the SSSA leading the SSA100 averaged in the center of the warm "Blob", and the right panels are the SSA leading the SSA100 averaged in the center of warm "Blob" anomaly. The colored areas passed the 0.05 significance test.

back effect of the oceanic physical process on the SSTA. The negative FWF anomaly leads to low salinity, stabilizes the upper ocean and then reduces the mixing and entrainment of the subsurface water. Consequently, the loss of surface heat can be reduced or prevented, and then, the SST will become higher. The negative SA in the NEP was very important to the appearance of the warm "Blob". For example, prior to the mature state of the warm "Blob", the negative SA occupied the surface and the depth

range of 100–150 m in the warm "Blob" region. The largest negative SA appeared in the depth range of 100–150 m and reached a value of -0.2. The anomaly was leading the warm "Blob" by approximately 12 months. In particular, the subsurface SA played a more important role in the shallowing of the MLD than the surface salinity and was important to increasing the SST of the warm "Blob" by inhibiting the heat from penetrating into the deeper layer. This large sea salinity vertical distribution feature in the

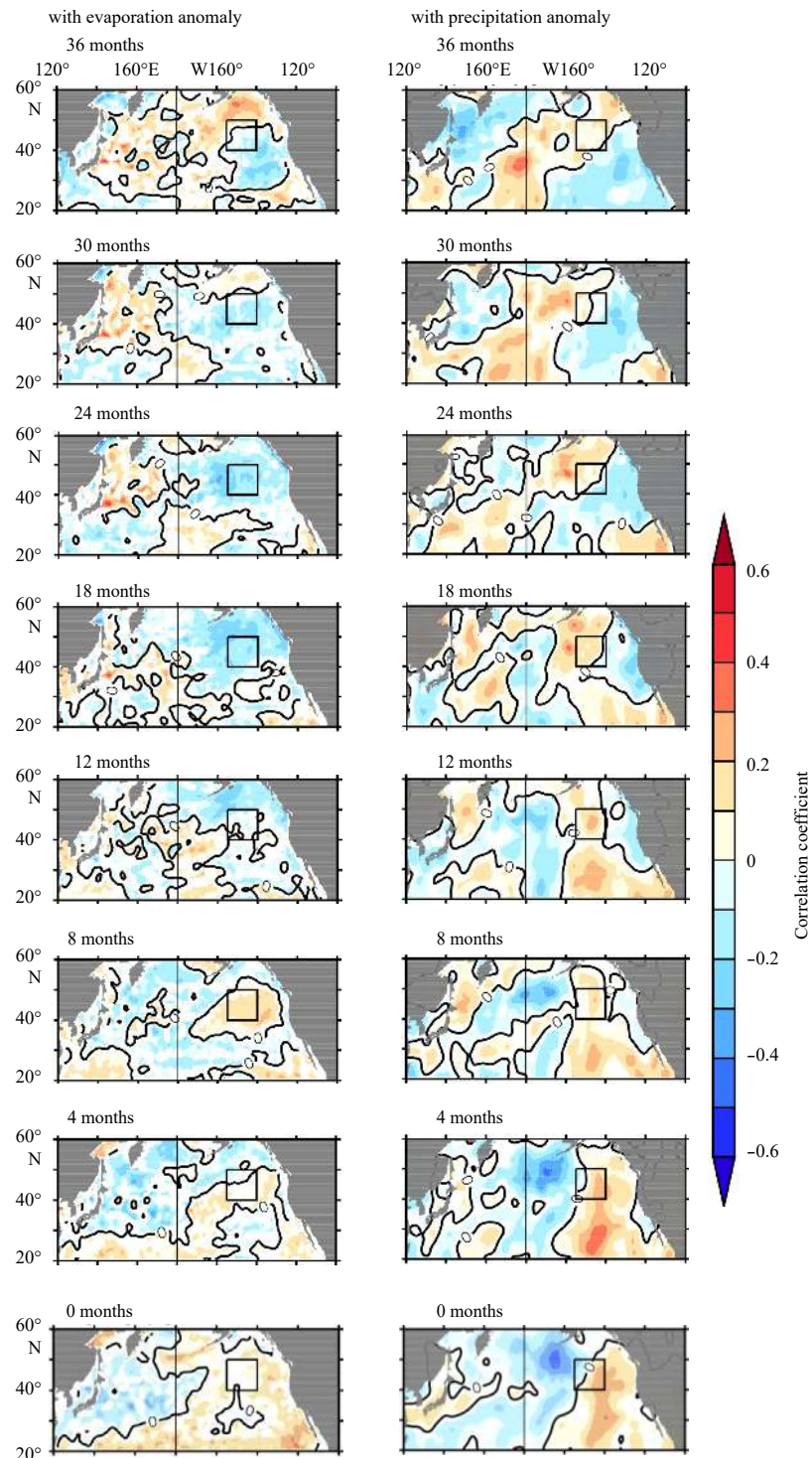


**Fig. 10.** The spatial distribution of the correlation coefficients showing that the evaporation anomaly leads the SSA at 100 m averaged in the center of the warm “Blob” from 36–0 months (left panels); the right panels are same as the left panels, but for the precipitation anomaly leading the SSA at 100 m averaged in the center of the warm “Blob”. The colored areas passed the 0.05 significance test.

upper ocean of the northern Pacific suggests a physical process that is obviously different from that in the tropical Pacific. Based on the above analyses, we can infer that the prior subsurface SA in the warm “Blob” region was more favorable to the adjustment of the density stratification at the base of the ML, which led to the change in the MLD by advection and diffusion rather than being effected by surface salinity.

The subsurface SA was mainly nonlocal and converged by ho-

zontal advection from the westward and southward areas. The westward and southward salinity anomalies were induced by the FWF anomaly. The anomaly can be enhanced near the dateline by the FWF anomaly. The FWF anomaly reduced the eastward transport of the salt water mass by the wind-driven gyre and increased the fresh water to the NEP across the dateline, which was associated with the atmospheric variability in the northern Pacific. The atmospheric variability was connected to the tropical

Pacific by a teleconnection, for instance, the weak 2014/2015 El Niño (di Lorenzo and Mantua, 2016). Through this teleconnection, the warm “Blob” event can influence the decadal variability in the northern Pacific, and thus, the variability exhibits the ocean-atmosphere coupled effect (Yoon et al., 2015; Whitney, 2015; di Lorenzo et al., 2015).

The warm “Blob” was an extreme climate event in the northern Pacific during 2005–2015. Notably, the warm “Blob” was analyzed and explained in many ways to understand its mechanism and the physics changes related to the warm “Blob” event, as well as the relationship between the characteristics and climate change. Hence, inspired by the heat budget of the mixed layer anomaly related to the warm “Blob” mentioned by Bond et al. (2015), we attempted to analyze the relationship between the SA and MLD change to explain the cause of the warm “Blob”’s appearance. Due to the ocean salinity observation limitations, many uncertainties about the salinity variability remained in association with the climate anomaly in the northern Pacific. In addition, the salinity and temperature distributions of the middle-high latitudes in the northern hemisphere were characterized by the formation and maintenance of the ocean stratifications, which were different from those in the tropical regions (Liu et al., 2009). The relevant theories of the tropical low latitudes may not fully explain the climatic phenomena in the high latitudes (Freeland et al., 1997; Johnson et al., 2016). For example, the mechanism of the salinity anomalies in response to the climate variability in PDO-related atmospheric forcing has not been fully resolved. In addition, the impact of the salinity decadal variability in the northern Pacific remains an open issue. Thus, it is reasonable that the SA in the northern Pacific may alter the warm “Blob”’s thermocline structure and stratification, and thus may affect the heat budget.

It is well known that the ocean salinity is not the main cause of the change in SST, and the ocean salinity indirectly affects only the SST and modulates ocean variability. However, the internal changes are interrelated and mutually influential in the climate system. The main purpose of this paper was to analyze the relationship between salinity and the ocean physical field and we attempted to analyze the presignal from the salinity perspective. As a precursor of the warm “Blob” event, the salinity can predict a climate anomaly. In general, the ocean heat budget may mainly lead to such events, and similar to the analysis by Bond et al. (2015), we will further analyze the heat budget in relation to the warm “Blob”.

The prediction of extreme climate change in the midlatitudes remains a challenge (Hu et al., 2017). The salinity does not play a direct role in the atmosphere. It was easier to obtain the origin of extreme climate change by tracing the SA than by tracing the temperature anomaly. Adding the salinity role into the coupled climate models can improve the prediction skills of ENSO (Ballabrera-Poy et al., 2002; Hackert et al., 2011; Zhao et al., 2013; Zhu et al., 2014). Our study showed that the SA likely played a role in affecting the extreme warm SSTA during the winter of 2013 in the NEP. Thus, based on the sustained ARGO observations combined with high-resolution numerical model outputs, it is necessary to contain the salinity effects in the prediction of extreme SST anomalies in the mid and high latitudes in the future.

#### Acknowledgements

Thanks for the suggestions and comments from two reviewers. We are thankful to ocean data providers such as IPRC (Argo data) and APDRC, NOAA, etc., and FERRET using graphical presentation.

#### References

- Adler R F, Huffman G J, Chang A, et al. 2003. The version-2 global precipitation climatology project (GPCP) monthly precipitation analysis (1979–present). *Journal of Hydrometeorology*, 4(6): 1147–1167, doi: [10.1175/1525-7541\(2003\)004<1147:TVGPP-CP>2.0.CO;2](https://doi.org/10.1175/1525-7541(2003)004<1147:TVGPP-CP>2.0.CO;2)
- Ballabrera-Poy J, Murtugudde R, Busalacchi A J. 2002. On the potential impact of sea surface salinity observations on ENSO predictions. *Journal of Geophysical Research*, 107(C12): 8007, doi: [10.1029/2001JC000834](https://doi.org/10.1029/2001JC000834)
- Baxter S, Nigam S. 2015. Key role of the north Pacific oscillation-west Pacific pattern in generating the extreme 2013/14 North American winter. *Journal of Climate*, 28(20): 8109–8117, doi: [10.1175/JCLI-D-14-00726.1](https://doi.org/10.1175/JCLI-D-14-00726.1)
- Blunden J, Arndt D S. 2015. State of the Climate in 2014. *Bulletin of the American Meteorological Society*, 96(7): ES1–ES32, doi: [10.1175/2015BAMSStateoftheClimate.1](https://doi.org/10.1175/2015BAMSStateoftheClimate.1)
- Bond N A, Cronin M F, Freeland H, et al. 2015. Causes and impacts of the 2014 warm anomaly in the NE Pacific. *Geophysical Research Letters*, 42(9): 3414–3420, doi: [10.1002/2015GL063306](https://doi.org/10.1002/2015GL063306)
- Bosc C, Delcroix T, Maes C. 2009. Barrier layer variability in the western Pacific warm pool from 2000 to 2007. *Journal of Geophysical Research*, 114(C6): C06023, doi: [10.1029/2008JC005187](https://doi.org/10.1029/2008JC005187)
- de Boyer Montegut C, Madec G, Fischer A S, et al. 2004. Mixed layer depth over the global ocean: an examination of profile data and a profile-based climatology. *Journal of Geophysical Research*, 109(C12): C12003, doi: [10.1029/2004JC002378](https://doi.org/10.1029/2004JC002378)
- di Lorenzo E, Liguori G, Schneider N, et al. 2015. ENSO and meridional modes: a null hypothesis for Pacific climate variability. *Geophysical Research Letters*, 42(21): 9440–9448, doi: [10.1002/2015GL066281](https://doi.org/10.1002/2015GL066281)
- di Lorenzo E, Mantua N. 2016. Multi-year persistence of the 2014/15 north pacific marine heatwave. *Nature Climate Change*, 6: 1042–1047, doi: [10.1038/nclimate3082](https://doi.org/10.1038/nclimate3082)
- Fedorov A V, Pacanowski R C, Philander S G, et al. 2004. The effect of salinity on the wind-driven circulation and the thermal structure of the upper ocean. *Journal of Physical Oceanography*, 34(9): 1949–1966, doi: [10.1175/1520-0485\(2004\)034<1949:TEO-SOT>2.0.CO;2](https://doi.org/10.1175/1520-0485(2004)034<1949:TEO-SOT>2.0.CO;2)
- Freeland H, Denman K, Wong C S, et al. 1997. Evidence of change in the winter mixed layer in the Northeast Pacific Ocean. *Deep Sea Research Part I: Oceanographic Research Papers*, 44(12): 2117–2129, doi: [10.1016/S0967-0637\(97\)00083-6](https://doi.org/10.1016/S0967-0637(97)00083-6)
- Freeland H, Whitney F. 2014. Unusual warming in the Gulf of Alaska. *Pices Press*, 22(2): 51–52
- Hackert E, Ballabrera-Poy J, Busalacchi A J, et al. 2011. Impact of sea surface salinity assimilation on coupled forecasts in the tropical Pacific. *Journal of Geophysical Research*, 116(C5): C05009, doi: [10.1029/2010JC006708](https://doi.org/10.1029/2010JC006708)
- Hartmann D L. 2015. Pacific sea surface temperature and the winter of 2014. *Geophysical Research Letters*, 42(6): 1894–1902, doi: [10.1002/2015GL063083](https://doi.org/10.1002/2015GL063083)
- Hu Zengzhen, Kumar A, Jha B, et al. 2017. Persistence and Predictions of the Remarkable Warm Anomaly in the Northeastern Pacific Ocean during 2014–16. *Journal of Climate*, 30(2): 689–701, doi: [10.1175/JCLI-D-16-0348.1](https://doi.org/10.1175/JCLI-D-16-0348.1)
- Huang Boyin, Mehta V M. 2005. Response of the Pacific and Atlantic oceans to interannual variations in net atmospheric freshwater. *Journal of Geophysical Research*, 110(C8): C08008, doi: [10.1029/2004JC002830](https://doi.org/10.1029/2004JC002830)
- Johnson B K, Bryan F O, Grodsky S A, et al. 2016. Climatological annual cycle of the salinity budgets of the subtropical maxima. *Journal of Physical Oceanography*, 46(10): 2981–2994, doi: [10.1175/JPO-D-15-0202.1](https://doi.org/10.1175/JPO-D-15-0202.1)
- Kara A B, Rochford P A, Hurlburt H E. 2000. An optimal definition for ocean mixed layer depth. *Journal of Geophysical Research*, 105(C7): 16803–16821, doi: [10.1029/2000JC900072](https://doi.org/10.1029/2000JC900072)
- Kintisch E. 2015. The Blob’ invades pacific, flummoxing climate experts. *Science*, 348(6230): 17–18, doi: [10.1126/science.348.6230.17](https://doi.org/10.1126/science.348.6230.17)
- Liu Hailong, Grodsky S A, Carton J A. 2009. Observed subseasonal

- variability of oceanic barrier and compensated layers. *Journal of Climate*, 22(22): 6104–6119, doi: [10.1175/2009JCLI2974.1](https://doi.org/10.1175/2009JCLI2974.1)
- Liu Lingling, Huang Ruixin. 2012. The global subduction/obduction rates: their interannual and decadal variability. *Journal of Climate*, 25(4): 1096–1115, doi: [10.1175/2011JCLI4228.1](https://doi.org/10.1175/2011JCLI4228.1)
- Palmer T. 2014. Record - breaking winters and global climate change. *Science*, 344(6186): 803–804, doi: [10.1126/science.1255147](https://doi.org/10.1126/science.1255147)
- Sprintall J, Tomczak M. 1992. Evidence of the barrier layer in the surface layer of the tropics. *Journal of Geophysical Research*, 97(C5): 7305–7316, doi: [10.1029/92JC00407](https://doi.org/10.1029/92JC00407)
- Tseng Y H, Ding Ruiqiang, Huang Xiaomeng. 2017. The warm Blob in the northeast Pacific—the bridge leading to the 2015/16 El Niño. *Environmental Research Letters*, 12(5): 054019, doi: [10.1088/1748-9326/aa67c3](https://doi.org/10.1088/1748-9326/aa67c3)
- van Oldenborgh G J, Haarsma R, de Vries H, et al. 2015. Cold extremes in North America vs. mild weather in Europe: the winter of 2013–14 in the context of a warming world. *Bulletin of the American Meteorological Society*, 96(5): 707–714
- Wang S Y, Hipps L, Gillies R R, Yoon J H. 2014. Probable causes of the abnormal ridge accompanying the 2013–2014 California drought: ENSO precursor and anthropogenic warming footprint. *Geophysical Research Letters*, 41(9): 3220–3226, doi: [10.1002/2014GL059748](https://doi.org/10.1002/2014GL059748)
- Whitney F A. 2015. Anomalous winter winds decrease 2014 transition zone productivity in the NE Pacific. *Geophysical Research Letters*, 42(2): 428–431, doi: [10.1002/2014GL062634](https://doi.org/10.1002/2014GL062634)
- Williams A P, Seager R, Abatzoglou J T, et al. 2015. Contribution of anthropogenic warming to California drought during 2012–2014. *Geophysical Research Letters*, 42(16): 6819–6828, doi: [10.1002/2015GL064924](https://doi.org/10.1002/2015GL064924)
- Yoon J H, Wang S Y S, Gillies R R, et al. 2015. Increasing water cycle extremes in California and in relation to ENSO cycle under global warming. *Nature Communications*, 6: 8657, doi: [10.1038/ncomms9657](https://doi.org/10.1038/ncomms9657)
- Yu L S, Jin X Z, Weller R A. 2008. Multidecade global flux datasets from the objectively analyzed air-sea fluxes (OAFlux) Project: latent and sensible heat fluxes, ocean evaporation, and related surface meteorological variables. Massachusetts: Woods Hole Oceanographic Institution, 64
- Yu Bin, Zhang Xuebin. 2015. A physical analysis of the severe 2013/2014 cold winter in North America. *Journal of Geophysical Research*, 120(19): 10149–10165, doi: [10.1002/2015JD023116](https://doi.org/10.1002/2015JD023116)
- Zhang Ronghua, Busalacchi A J. 2009. Freshwater flux (FWF)-induced oceanic feedback in a hybrid coupled model of the tropical Pacific. *Journal of Climate*, 22: 853–879, doi: [10.1175/2008JCLI2543.1](https://doi.org/10.1175/2008JCLI2543.1)
- Zhang Ronghua, Gao Chuan, Kang Xianbiao, et al. 2015. ENSO modulations due to interannual variability of freshwater forcing and ocean biology-induced heating in the tropical Pacific. *Scientific Reports*, 5: 18506, doi: [10.1038/srep18506](https://doi.org/10.1038/srep18506)
- Zhang Ronghua, Wang Guihua, Chen Dake, et al. 2010. Interannual biases induced by freshwater flux and coupled feedback in the tropical Pacific. *Monthly Weather Review*, 138(5): 1715–1737, doi: [10.1175/2009MWR3054.1](https://doi.org/10.1175/2009MWR3054.1)
- Zhao Mei, Hendon H H, Alves O, et al. 2013. Impact of salinity constraints on the simulated mean state and variability in a coupled seasonal forecast model. *Monthly Weather Review*, 141(1): 388–402, doi: [10.1175/MWR-D-11-00341.1](https://doi.org/10.1175/MWR-D-11-00341.1)
- Zheng Fei, Zhang Ronghua. 2012. Effects of interannual salinity variability and freshwater flux forcing on the development of the 2007/08 La Niña event diagnosed from Argo and satellite data. *Dynamics of Atmospheres and Oceans*, 57: 45–57, doi: [10.1016/j.dynatmoce.2012.06.002](https://doi.org/10.1016/j.dynatmoce.2012.06.002)
- Zheng Fei, Zhang Ronghua, Zhu Jiang. 2014. Effects of interannual salinity variability on the barrier layer in the western-central equatorial Pacific: A diagnostic analysis from Argo. *Advances in Atmospheric Sciences*, 31: 532–542, doi: [10.1007/s00376-013-3061-8](https://doi.org/10.1007/s00376-013-3061-8)
- Zhu Jieshun, Huang Bohua, Zhang Ronghua, et al. 2014. Salinity anomaly as a trigger for ENSO events. *Scientific Reports*, 4: 6821, doi: [10.1038/srep06821](https://doi.org/10.1038/srep06821)